INDIAN JOURNAL OF SCIENCE AND TECHNOLOGY

RESEARCH ARTICLE

Check for updates

OPEN ACCESS

Received: 19-09-2021

Accepted: 24-02-2022

Published: 09.04.2022

Citation: Ouédraogo S, Ousmane M, Mogmenga L, Sikoudouin Maurice Ky T, Kam S, Bathiébo J (2022) Experimental Study of the Airflow in Natural Convection in an Innovative Prototype of Solar Chimney Power Plant, under Climatic Conditions in Ouagadougou, Burkina Faso. Indian Journal of Science and Technology 15(14): 619-629. https://doi.org/10.17485/IJST/v15i14.1737

* **Corresponding author**.

osalif12@gmail.com

Funding: We are grateful to the International Science Program (ISP) for supporting BUF01

Competing Interests: None

Published By Indian Society for Education and Environment (iSee)

ISSN
Print: 0974-6846
Electronic: 0974-5645

Experimental Study of the Airflow in Natural Convection in an Innovative Prototype of Solar Chimney Power Plant, under Climatic Conditions in Ouagadougou, Burkina Faso

Salifou Ouédraogo[1]*, Moctar Ousmane[2], Ladifata Mogmenga[1], Thierry Sikoudouin Maurice Ky, Sié Kam[1], Joseph Bathiébo[1]

1 Laboratory L.E.T.RE, University and KIZERBO, Ouagadougou 03, 7021, Burkina Faso
2 University of Agadez, 199, Niger

Abstract

Objectives: In sunny regions, chimney solar power plants are a promising technology because they depend mainly on solar energy. However, chimney solar power plants require an optimal design of the power plant components to improve its reliability and scalability. As the collector is one of the essential components of the solar chimney power plant, this study presents an experimental study that aims to improve the thermo-aerodynamic parameters of the airflow involved. **Methods**: We used mini hemispherical concentrators in the collector as an innovation and the experimental conditions are those of a dry tropical zone during the dry season. Temperature and velocity were measured during a measurement campaign. **Findings**: The analysis of the results showed an improvement of the thermo-aerodynamic parameters, in particular the air temperature in the collector and its velocity in the chimney, with maximum values reaching 78.35 °C and 2.87 m/s respectively. We also note an improvement of the thermal field of 24.4 % and the dynamic field of 58.6% compared to a conventional solar chimney model of the same dimensions. A thermal efficiency of 68.88 % was achieved. These values highlight the innovation relevance and the performance improvement of the solar chimney prototype.

Keywords: Experimentation; Airflow; Natural Convection; Solar Chimney Power Plant; Hemispherical Reflector

1 Introduction

Solar energy is the most available and accessible renewable energy in the very long term, B. Bendaoud et al.[1] and A. Rishak et al. in[2]. This energy is exploited for various purposes, the most common use of which in practice is in thermal and electrical domain. Thermal systems, through solar collectors, convert solar rays into heat which is transmitted directly or indirectly to a heat transfer fluid [3]. On the one hand, electrical systems refer to the direct conversion of solar radiation into electrical energy, through photovoltaic cells [4]. On the other hand, there are technologies that use the operating principle of thermal systems to produce electricity. One of them being the Solar Chimney Power Plants (SCPP) which is the subject of this study. In fact the first solar chimney power plant prototype was built in Manzanares (Spain) in 1982 with a nominal power of 50 kW and operated successfully for seven years, from 1982 to 1989 [5]. This technology is mainly composed of a collector, a chimney and a turbine, with an operating principle based on the force of an ascending air stream [6]. Studies conducted on the operation of the pilot plant have shown the feasibility of this technology but also a low efficiency in operation [7]. The results have sparked a research craze for this technology and a particular interest in improving its performance. To ensure the continuity of the SCPP's production at night and in intermittent periods, Kreetz [5], proposed to fix water-filled black tubes side by side on the ground absorbing's the radiation under the collector. As for Omar et al. [6], they integrated geothermal water in coils on the ground under the collector. These proposals resulted, on one hand, in the improvement of the SCPP's performance in the solar radiation presence, and on the other hand, in the production continuity.

Results of experimental [7–9] and theoretical [10–12] studies carried out on SCPP prototypes have shown that the most influential parameters are the diameter of the collector, the height and the diameter of the chimney and the solar radiation. The results of a study conducted by Mehdipour et al. [13] showed that the higher these parameters are, the higher the SCPP performance get. Thus, it is apparent that the SCPP is technically cost-effective only on a large scale.

Authors such as Ayadi et al. [14], Ghalamchi et al. [15], Setareh et al. [16] demonstrated that the inclination of the collector roof is a parameter that has an impact on the air flow in the system. However, positive and negative tilts do not have the same impact. The well-discussed results of Mehdipour et al. [17] showed that a positive manifold tilt angle controls the formation of secondary flows. Moreover, this slope facilitates the cleaning of the roof and avoids the accumulation of rainwater. The inlet cross-section of the collector should be optimized to mitigate the effect of wind speed on the transfer coefficients in the collector [18,19]. A geometry of a solar chimney was proposed by Arzpeyma et al. [20], to minimize the negative effects of wind at the collector inlet and at the chimney outlet.

Wang et al. [21] showed that when the thermal efficiency of the collector is high, the SCPP performance is better. It was found that under windy conditions, tilted or floating solar chimneys have better flow and resistance performance compared to the fixed chimneys [22,23].

Some authors have also focused on the turbine, which is also one of the main components to operate the SCPP. The turbine is regulated according to the pressure drop and not according to the speed like a wind turbine. Koonsrisuk et al. [24], Kirstein et al. [25], Gannon et al. [26] have shown that for a constant heat flow, the power of the flow is at the maximum level in the turbine when the pressure drop is higher.

Technical and economic analyses have been carried out by Saleheen et al. [27] and Zuo et al. [28] on the SCPP. It stemmed from this analysis that this technology is only economically viable on a large scale and therefore needs a significant subsidy to make it competitive. To address this concern, Ali et al. [29] proposed economical models of solar chimneys under favorable climatic conditions. These models relate the geometrical dimensions to the production capacity. The data of the models are as follows Table 1.

Table 1. Solar tower dimensions as a function of production capacity [29]

Capacity (MW)	5	30	100	200
H_{ch} (m)	550	750	1000	1000
D_{ch} (m)	45	70	110	120
D_c (m)	1250	2900	4300	7000

Analyzing the partial results obtained in the literature, the hypothesis put forward by Liu et al. [30] remains a reality. According to the same authors, the energy production capacity improvement of the SCPP would be shrewd, if it didn't increase the height of the chimney and the collector surface. In this perspective, our work consists in improving the collector performance. Our previous studies allowed us to develop a model of collector with satisfactory thermal performances [31,32]. This article is a continuation of our previous work, we will experimentally analyze the thermo-aerodynamic behavior of the air flow in our prototype as well as the relevance of this innovation. For so doing, we will measure the temperature and velocity in the system. And then, we will analyze and discuss the relevance of the study in the SCPP's field.

2 Materials and methods

2.1 Description of the prototype

The experimental model was designed at the Thermal Renewable Energies Laboratory (L.E.T.RE) of Université Joseph KI-ZERBO of Ouagadougou, Burkina Faso. We used Autocad 2018 software to represent the 3D sketch of the model before its physical design. The sketch diagram is shown in Figure 1, where fixed mini hemispheric concentrators are housed in the model manifold and an absorber occupies the interstitial space between the hemispheres.

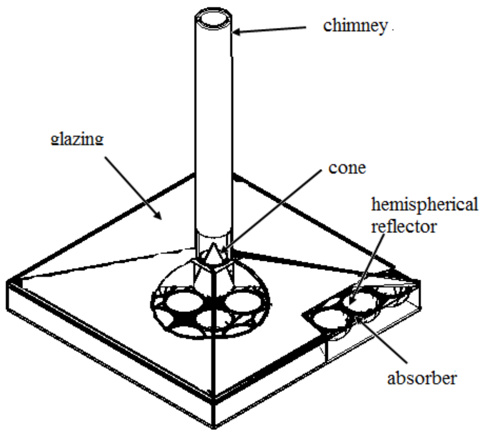

Fig 1. Model schematic of the solar chimney prototype.

Truncations were made on the glass to make the hemispheric concentrators, the absorber and the diffuser visible. The picture of the experimental device is shown in Figure 2.

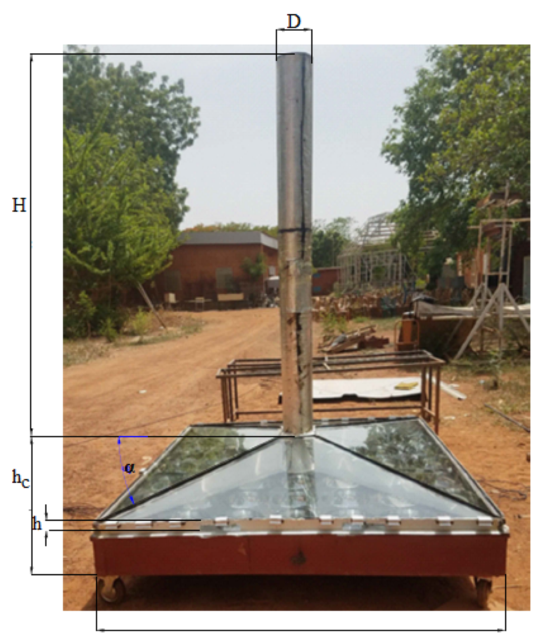

Fig 2. Picture of the experimental model

The chimney is made of 3 mm thick mild steel and insulated with TRAPALU-40, which minimizes the possible loss of the captured heat flows by convection and radiation. The collector, housing hemispherical concentrators of 28 cm diameter for each hemisphere, is made of a 5 mm thick transparent soda-lime glass roof. The square collector has a side of 2 m, which is a collection surface of 4 m^2. In the following we will use the term "radius" the value of which is 1.13 m than the side, for the same surface of the collector. The pane is positively inclined at an angle of 9° along a radius from the periphery to the center. Mehdipour et al [17] proposed a positive tilt of the roof in the range of 0° to 14° to reduce heat loss. The hemispheres of our system are a reuse of IKEA BLANDA BLANK salad bowls of 280 mm diameter. These bowls are made of stainless steel and have a reflective chrome interior surface. As stated above, this work is a continuity and the modifications made on the prototype are the inclination of the roof, the presence of the diffuser and the reduction of the air inlet section in the collector.

Inside each hemisphere, a hot spot is formed whose existence depends on the sunshine. The hot spot is the image of the sun at the focal point of the hemisphere. The picture of a hemisphere and the principle of the hot spot in the hemisphere are shown in Figure 3.

The advantage of using hemispheric concentrators is that they always concentrate the solar radiation inside hemisphere at any time [33]. This minimizes the costs associated with the system maintenance.

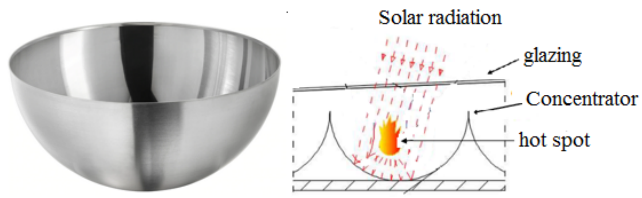

Fig 3. Picture of a hemisphere and the hot spot principle inside the hemisphere.

Table 2 shows the geometric dimensions of the solar chimney prototype.

Table 2. Geometric parameters of the solar chimney prototype

	Collector					Chimney	
Parameters	c(m)	h_c(m)	h(m)	α(°)	Hemisphere r(m)	H(m)	D(m)
	2	0.2	0.05	9°	0.14	2	0.2

2.2 Experimental protocol

We carried out an experimental campaign at the Central Maintenance Workshop (ACM) of Université Joseph KI-ZERBO. This campaign consisted in measuring:

- The temperature of the absorber and of the air in the collector as well as in the chimney;
- The air velocity in the stack; and
- The global solar radiation on a horizontal plane.

For this purpose, the equipment and measurement methods used are listed below:

- Type K thermocouples with external shielding for temperature measurement,
- A Hukseflux SR03-05 pyranometer to measure global irradiation,
- Two GRAPHTEC Midi LOGGER GL200A data loggers programmed with the pyranometer and thermocouples, three hot-wire anemometers (testo 480 automatic logger, testo 425 and HVACR Datalogger DO2003 manual logger). Technical description of the measuring instruments is given in Table 3.

The average air temperature at a point on the collector is obtained by averaging the temperatures measured by two thermocouples that are distinctly placed in the vertical of the point. Let bi and hi be the points on the same vertical; i=0; 1; 2; 3, the average air temperature at a point is given by equation 1. These thermocouples are not in contact with the glass or the absorber.

$$T_i = \frac{T_{h_i} + T_{b_i}}{2} \tag{1}$$

Table 3. Measuring range and accuracy of measuring equipment

Instrument		Measuring range	Accuracy
Thermocouples of K type		-100°C – 370°C	± (0.1% of reading + 0.3°C)
A pyranometer SR03-05 of Hukse flux brand sensibility=9.58 μV (W.m^{-2})		0 – 2000 W/m^2	± 15 W/m^2
A hot wire anemometer	Model Testo 425 (manual) Model Testo 480 (Automatic)	0– 20 m/s	± (0.03 m/s + 5 % v.m.)
Anemometer HVACR Datalogger DO2003((manual)		0.25 – 20 m/s	±0.2 m/s (0.25 - 19.99 m/s)

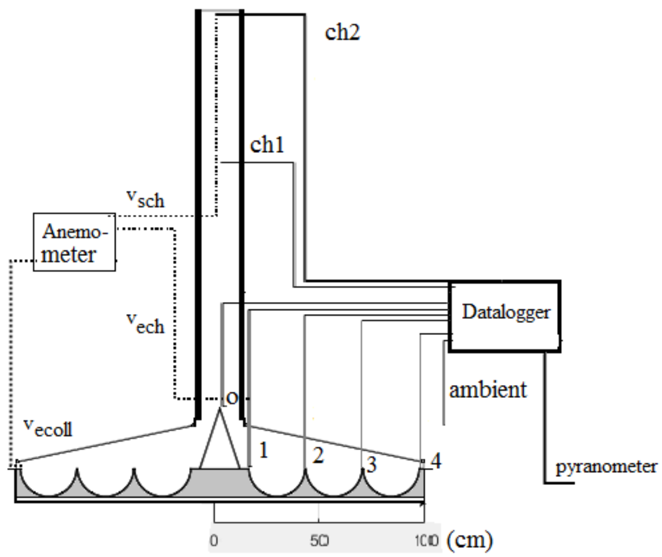

Fig 4. Location of thermocouples and velocity probes.

The temperature of the absorber at a point is measured by placing the thermocouple in contact with the absorber. The measurements on the absorber concerned the points 1; 2 and 3 in Figure 4.

Data are saved in CSV file format and then imported into matlab 2018.a software for curve plotting.

This campaign took place in the months of April, May and June of 2020, according to the days listed in Table 4.

Table 4. Measurement period

Month	Measurement day
April	07 ; 15 ; 17
May	07 ; 15 ; 17
June	05 ; 08 ; 11

3 Results and discussion

The maximum values of some parameters from four (4) measurement days are given in Table 5. In this table G is the solar radiation, ΔT is the temperature difference of the air in the collector ($\Delta T = T_0 - T_4$) and V_{ech} is the air velocity at the stack inlet.

A comprehensive analysis of these values shows that the higher the temperature difference (ΔT) and radiation, the higher the air speed. This has already been established in the literature.

In order to analyze our results in detail, on the data of June 11, 2020 will be presented.

Table 5. Maximum values of several parameters

Day	G(W/m^2)	ΔT (°C)	Vech (m/s)
April 07, 2020	957	41.2	1.98
April 14, 2020	908	38	1.75
May 07, 2020	973.3	41.3	2.80
June 11, 2020	941.8	43.5	2.87

3.1 Evolution of temperature and global radiation

Figure 5 shows the evolution of the global solar radiation and the ambient temperature at the measurement site. The solar radiation curves have a parabolic evolution and reach their maximum values of 941.8 W/m^2 at 11:44 am. The evolution of solar radiation and ambient temperature show jumps in values caused by load shedding at the measurement site.

The ambient temperature reaches its maximum value of 37.8 °C at 3:12 pm.

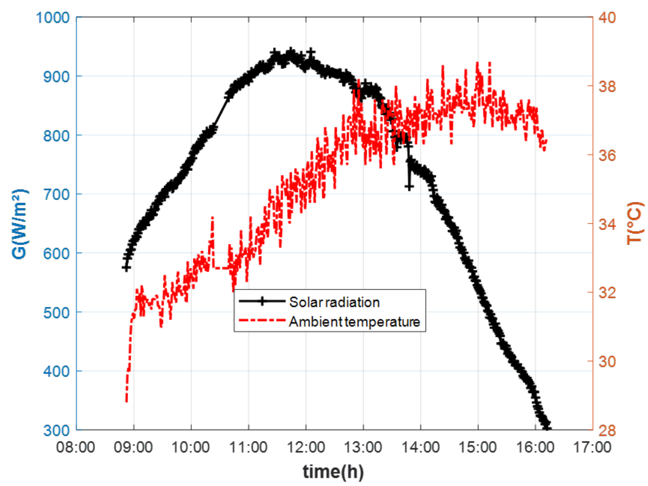

Fig 5. Temporal evolution of global radiation and ambienttemperature

Figures 6 and 7 shows the temporal and spatial evolution of the temperature at the different measurement points inside the prototype.

The temporal evolution of the temperature represented in Figure 6.a), b) and c), shows maximum values 91.7 °C at 12:20 pm; 78.35 °C at 12:46 pm and 64.5 °C 12:48 reached respectively by the absorber, the air inside the collector and the chimney outlet. These curves show similar patterns as the solar radiation. The time difference between the different peaks reflects the time needed to reach thermal equilibrium in the collector, which depends on the thermal inertia of the collector materials.

Compared to the average air temperature of 56°C obtained in our previous study[31], the average air temperature obtained in this study has been improved to 62 °C. The reduction of the air inlet section in the collector has contributed to reducing the heat losses in the proximity of this section.

We found out that as the solar radiation curve decreases, the temperature in the prototype decreases too. Nouar et al.[34] have established the same observation by studying the effects of climate on the performance of solar chimney power plants.

Figure 7 is obtained by taking for each measurement point, three temperature values at different times.

In space of the collector, the temperatures of the absorber (Figure 7a) and the air (Figure 7b) increase from the periphery (point 4) to the center (point 1) of the collector. At measuring point 1 the temperatures are higher. We also see a drop in air temperature at the chimney entrance, point 0. Indeed, at the chimney entrance, the widening of the cross-section due to the roof slope increases the volume of air to be heated. In addition, the thermal energy acquired by the air is converted into kinetic energy. The temperature of the air in the chimney (Figure 7c) decreases from the inlet to the outlet, which proves that the insulation of the chimney prevents the heat exchange of the external environment with the walls. All these observations have been established by many authors[35].

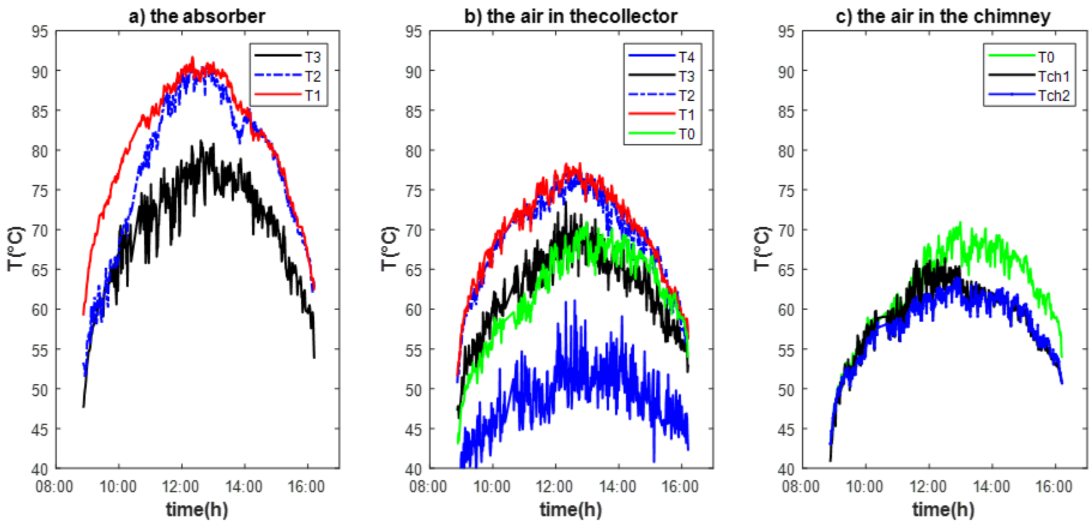

Fig 6. Temporal evolution of temperature a) of the absorber, b) of the air in collector and c) of the air in the chimney

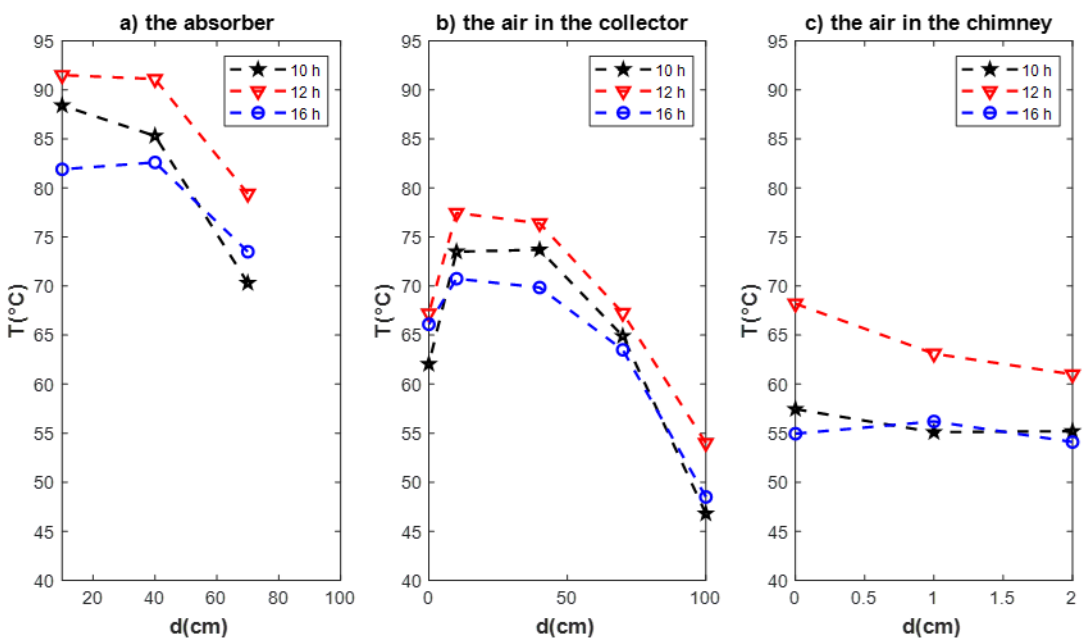

Fig 7. Temporal evolution of temperature a) of theabsorber, b) of the air in collector and c) of the air in the chimney.

3.2 Evolution of air velocity

The evolution of air velocities at the inlet of the collector, at the inlet and at the outlet of the 2 m high chimney and of the thermal efficiency is represented by Figure 8. The curves show the important fluctuations in the measurement period with respective maximum values of 0.8 m/s, 2.87 m/s, 1.6 m/s and 0.6888 or 68.88 %. The evolution of the air velocity at the entrance as well as at the exit of the stack is more important between 9 am and 2.30 pm and the velocity is higher at the entrance than at the exit.

As the temperature difference increases, the air density difference also increases, inducing a significant thermosiphon effect. This effect is more significant towards the outlet of the collector where the air temperatures are higher. The air in this area is also subject to the suction effect of the stack.

The coupling of the thermosyphon effect and the stack aspiration effect explains the large value of the velocity at the stack inlet. M. Ousmane et al.[36] showed by theoretical analysis that the air velocity is higher in the stack in the area near its entrance.

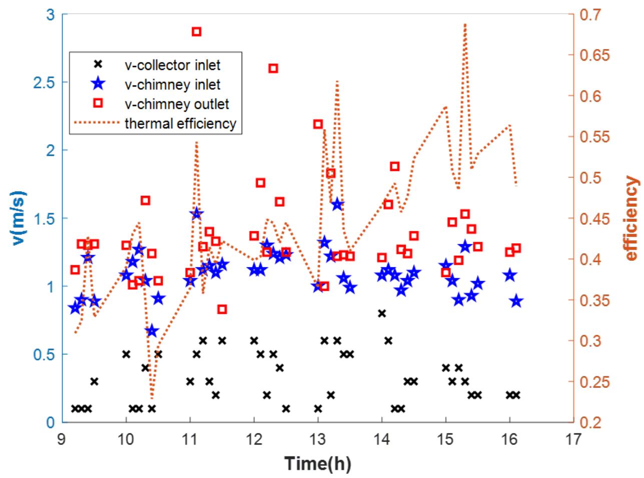

Fig 8. Temporal evolution of air velocity and thermalefficiency.

Using the Boussinesq approximation, Haaf et al.[37] established the equations for the theoretical air velocity in the stack under natural convection and for the collector efficiency:

$$V = \sqrt{2gH_{ch}\frac{\Delta\theta}{\theta_{amb}}} \quad (2)$$

$$\eta = \frac{\dot{m}C_p\Delta\theta}{A_cG} \quad (3)$$

$$m = \rho A_{ch}V_{ch} \quad (4)$$

The average efficiency value is estimated at 44.5%, which is higher than the maximum efficiency of 40 % that a flat plate solar collector with fixed air could achieve[38]. From the equations established by Haaf et al.[37] and the above observation, it follows that the higher the temperature difference, the greater the air velocity in the system. Our results are in agreement with these theoretical predictions. The modifications in the collector have thus contributed to the improvement of the collector thermal efficiency.

Some results from studies performed on the collector performance improvement of solar tower prototypes are mentioned in Table 6. A comparative analysis of this table will allow to locate the relevance of our work.

Table 6. Comparison with some works

Authors	Solar intensity enhancement method	Dc (m)	Hch (m)	Tmax(°C)	vmax (m/s)	G(W/m^2)
Khidhir et al. (Iraq)[39]	Tracking reflector mirror	9	7.35	54	2.4	616
A.Shahreza et al. (Iran)[40]	Tracking reflector mirror	0 .92	1.5	72	5.2	600
Balijepalli et al. (India)[7]	Improved flat absorber	3.5	6	67.5	5.5	894
Al-Kayiem et al.[41] (Malaysia)	Hybrid system	6	6.65	55	1.9	1086
Mehdipour et al. (Iran)[13]	Improved flat absorber	2.26	3	69.45	1.63	1000
Ouédraogo et al. (Burkina-Faso)[42]	Flat absorber	2.26	2	63	1.81	967
Present work	Stationary hemispherical reflector	2.26	2	78.35	2.87	941.75

The velocity and temperature values recorded in Table 6 show an improvement in thermal performance as a result of the different investigations. The values of the air velocity in the system are improved, certainly with the improvement of the thermal performance, but particularly because of the prototype dimensions. The value of the temperature reached by the air in the collector of our prototype, compared to the other values in the table highlights the relevance of the use of hemispherical reflectors in the collector of the prototype.

For the same dimensions, we recorded maximum values of temperature and velocity of 63°C; 1.81 m/s for a solar radiation of 967 W/m^2 with a conventional solar chimney prototype and 78.35°C; 2.87 m/s for a solar radiation of 941.75 W/m^2 with our prototype. We note an improvement of the thermal field of 24.4% and the dynamic field of 58.6%. These values highlight the relevance of the innovation and the improvement of the performances of the solar chimney prototype.

4 Conclusion

This study allowed us to take into account the velocity evolution for a more global analysis of the airflow in the system compared to our previous study. In addition, the decrease of the air inlet cross-section and the inclination of the collector roof (9°) were considered as major modifications. These modifications have contributed to reducing the heat backflow near the inlet section. The results of this study are generally in agreement with those obtained in the literature. The air in the system reached a maximum temperature difference between the outlet and the inlet of the collector of 43.5 °C and a maximum velocity of 2.87 m/s for a solar radiation of 941.75 W/m^2. We also note an improvement of the thermal field of 24.4% and the dynamic field of 58.6% compared to the conventional solar chimney model. In sum, we can say that the use of hemispherical concentrators is a way to improve the thermos-aerodynamic parameters, especially the temperature and air velocity in natural flow in solar chimney power plants.

It is clear to us that this innovation allows a higher and more direct control of the thermal field via the temperature of the flowing air stream than the dynamic field characterized by the air velocity.

5 Nomenclature

- A: area (m^2)
- T or θ: temperature (°C or (K)
- ΔT or $\Delta\Theta$: temperature difference (°C) or (K)
- v: air speed (m/s)
- g: gravity (m/s^2)
- Cp: heat capacity at constant pressure (J/ (K.kg))
- G: global radiation (W/m^2)
- H: height of chimney (m)
- D: Diameter of chimney (m)
- h: Inlet height of the collector (m)
- h_c: height of the collector (m)
- c: Side of the collector (m)
- η: thermal efficiency of the collector
- ρ: air density (kg/m^3)
- r: radius of the hemisphere (m)
- α: tilt angle of the collector (°)
- amb: ambient
- ab: absorber
- c: collector
- max: maximum
- ch: chimney
- ech: chimney inlet
- sch: chimney outlet
- sc: collector outlet

6 Acknowledgement

We are grateful to the International Science Program (ISP) for supporting BUF01.

References

1) Bendaoud B, Malek A, Larbi L, Maammeur H. Conceptual study of photovoltaic power plant connected to the urban electrical network in northern Algeria. *Energy Sources, Part A : Recovery, Utilization and Environmental Effects*. 2020;2020:1–20. Available from: https://doi.org/10.1080/15567036.2020.1758852.
2) Rishak QA, Sultan HS, Jawad IN. Experimental Study of The Performance of a Solar Chimney Power Plant Model in Basrah City. *Journal of Mechanical Engineering Research and Developments*;2021:340–351. Available from: https://faculty.uobasrah.edu.iq/uploads/publications/1624955620.pdf.
3) Ouedraogo B, Dianda B, Palm K, Bahiebo D. Influence of Adding Rectangular Fins on the Performances of a Thermal Solar Air Plane Collector. *British Journal of Applied Science & Technology*. 2015;11(6):1–11. Available from: https://dx.doi.org/10.9734/bjast/2015/20741.
4) Zhou W, Yang H, Fang Z. A novel model for photovoltaic array performance prediction. *Applied Energy*. 2007;84(12):1187–1198. Available from: https://dx.doi.org/10.1016/j.apenergy.2007.04.006.
5) Too JHY, Azwadi CSN. A Brief Review on Solar Updraft Power Plant. *Journal of Advanced Review on Scientific Research*. 2016;18(1):1–25. Available from: https://www.akademiabaru.com/doc/ARSRV18_N1_P1_25.pdf.
6) Mokrani OBEK, Ouahrani MR, et Ladjel Segni MHS. Experimental investigations of hybrid: geothermal water/solar chimney power plant. *Energy Sources, Part A: Recovery, Utilization and Environmental Effects*. 2020;p. 1–18. Available from: https://doi.org/10.1080/15567036.2020.1810830.
7) Balijepalli R, Chandramohan VP, Kirankumar K. Development of a small scale plant for a solar chimney power plant (SCPP): A detailed fabrication procedure, experiments and performance parameters evaluation. *Renewable Energy*. 2020;148:247–260. Available from: https://dx.doi.org/10.1016/j.renene.2019.12.001.
8) Hassan AA, Ahmed OK, Abbas EF. Experimental Study of Performance of Solar Chimney. *IOP Conference Series: Materials Science and Engineering*. 2021;1094(1):012046. Available from: https://dx.doi.org/10.1088/1757-899x/1094/1/012046.
9) Arzpeyma M, Mekhilef S, Newaz KMS, Horan B, Seyedmahmoudian M, Akram N, et al. Solar chimney power plant and its correlation with ambient wind effect. *Journal of Thermal Analysis and Calorimetry*. 2020;141(2):649–668. Available from: https://dx.doi.org/10.1007/s10973-019-09065-z.
10) Cuce E, Sen H, Cuce PM. Numerical performance modelling of solar chimney power plants: Influence of chimney height for a pilot plant in Manzanares, Spain. *Sustainable Energy Technologies and Assessments*. 2020. Available from: https://doi.org/10.1016/j.seta.2020.100704.
11) Das P, Chandramohan VP. Effect of chimney height and collector roof angle on flow parameters of solar updraft tower (SUT) plant. *Journal of Thermal Analysis and Calorimetry*. 2019;136(1):133–145. Available from: https://dx.doi.org/10.1007/s10973-018-7749-y.
12) Das P, Chandramohan VP. 3D numerical study on estimating flow and performance parameters of solar updraft tower (SUT) plant: Impact of divergent angle of chimney, ambient temperature, solar flux and turbine efficiency. *Journal of Cleaner Production*. 2020;256:120353. Available from: https://dx.doi.org/10.1016/j.jclepro.2020.120353.
13) Mehdipour R, Baniamerian Z, Golzardi S, Murshed SMS. Geometry modification of solar collector to improve performance of solar chimneys. *Renewable Energy*. 2020;162:160–170. Available from: https://dx.doi.org/10.1016/j.renene.2020.07.151.
14) Ayadi A, Bouabidi A, Driss Z, Abid MS. Experimental and numerical analysis of the collector roof height effect on the solar chimney performance. *Renewable Energy*. 2018;115:649–662. Available from: https://dx.doi.org/10.1016/j.renene.2017.08.099.
15) Ghalamchi M, Kasaeian A, Ghalamchi M, Mirzahosseini AH. An experimental study on the thermal performance of a solar chimney with different dimensional parameters. *Renewable Energy*. 2016;91:477–483. Available from: https://dx.doi.org/10.1016/j.renene.2016.01.091.
16) Setareh M. Comprehensive mathematical study on solar chimney powerplant. *Renewable Energy*. 2021;175:470–485. Available from: https://dx.doi.org/10.1016/j.renene.2021.05.017.
17) Mehdipour R, Golzardi S, Baniamerian Z. Experimental justification of poor thermal and flow performance of solar chimney by an innovative indoor experimental setup. *Renewable Energy*. 2020;157:1089–1101. Available from: https://dx.doi.org/10.1016/j.renene.2020.04.158.
18) Shen W, Ming T, Ding Y, Wu Y, de_Richter RK. Numerical analysis on an industrial-scaled solar updraft power plant system with ambient crosswind. *Renewable Energy*. 2014;68:662–676. Available from: https://dx.doi.org/10.1016/j.renene.2014.03.011.
19) Weli RB, Atrooshi SA, Schwarze R. Investigation of the performance parameters of a sloped collector solar chimney model – An adaptation for the North of Iraq. *Renewable Energy*. 2021;176:504–519. Available from: https://dx.doi.org/10.1016/j.renene.2021.05.075.
20) Arzpeyma M, Mekhilef S, Newaz KMS, Horan B, Seyedmahmoudian M, Akram N, et al. Numerical simulation of the effect of chimney configuration on the performance of a solar chimney power plant. *Journal of Thermal Analysis and Calorimetry*. 2022;147(3):2549–2563. Available from: https://dx.doi.org/10.1007/s10973-021-10567-y.
21) Wang H, Chen J, Dai P, Zhang F, Li Q. Simulation and Experimental Study of the Influence of the Baffles on Solar Chimney Power Plant System. *Processes*. 2021;9(5):902–902. Available from: https://dx.doi.org/10.3390/pr9050902.
22) RahimiLarki M, Abardeh RH, Rahimzadeh H, Sarlak H. Performance analysis of a laboratory-scale tilted solar chimney system exposed to ambient crosswind. *Renewable Energy*. 2021;164:1156–1170. Available from: https://dx.doi.org/10.1016/j.renene.2020.10.118.
23) Arefian A, Abardeh RH. Ambient crosswind effect on the first integrated pilot of a floating solar chimney power plant: experimental and numerical approach. *Journal of Thermal Analysis and Calorimetry*. 2022;147(3):2803–2821. Available from: https://dx.doi.org/10.1007/s10973-021-10620-w.
24) Koonsrisuk A, Chitsomboon T. Theoretical turbine power yield in solar chimney power plants, editor. Thermal Issues in Emerging Technologies. In: and others, editor. 3rd International Conference on Thermal Issues in Emerging Technologies Theory and Applications. 2010. doi:https://doi.org/10.1007/s10973-021-10620-w.
25) Kirstein CF, von Backström TW. Flow Through a Solar Chimney Power Plant Collector-to-Chimney Transition Section. *Journal of Solar Energy Engineering*. 2006;128(3):312–317. Available from: https://dx.doi.org/10.1115/1.2210502.
26) Anthony J, Gannon TW, Backström. Solar Chimney Turbine: Part 1 of 2 : Design, In Conference ISE, Nevada, Solar Energy. In Conference ISE, Nevada, Solar Energy. 2002. Available from: https://asmedigitalcollection.asme.org/ISEC/proceedings/SED2002/16893/335/291271.
27) Saleheen RU, Rahman M, Mashud M, Paul S. Cold Inflow-Free Solar Chimney. Cold Inflow-Free Solar Chimney;vol. 2021. Singapore. Springer. 2021. Available from: http://dx.doi.org/10.1007/978-981-33-6831-6.
28) Zuo L, Liu Z, Qu N, Dai P, Sun Y, Qu B. Economic analysis of a wind supercharging solar chimney power plant combined with thermal plant for power and freshwater generation. *2020 12th IEEE PES Asia-Pacific Power and Energy Engineering Conference (APPEEC)*. 2020. Available from: https://ieeexplore.ieee.org/document/9220738/.
29) Ali B. Techno-economic optimization for the design of solar chimney power plants. *Energy Conversion and Management*. 2017;138:461–473. Available from: https://dx.doi.org/10.1016/j.enconman.2017.02.023.
30) Liu Q, Cao F, Liu Y, Zhu T, Liu D. Design and Simulation of a Solar Chimney PV/T Power Plant in Northwest China. *International Journal of Photoenergy*. 2018;2018:1–12. Available from: https://dx.doi.org/10.1155/2018/1478695.

31) Thierry SMK, Ouédraogo S, Ouédraogo A, Dianda B, Bathiébo MODJ, Ousmane M. Novel convection process : experimental study of a solar chimney with its collector made of hemispherical concentrator. *International journal of engineering sciences & research technology*. 2018;7(10):83–96. doi:10.5281/zenodo.1471587.
32) Ky TSM, Ouedraogo S, Ousmane M, Dianda B, Ouedraogo E, Bathiebo DJ. Experimental Study of a Stationary Hot Air Solar Collector Built with Hemispherical Concentrators and Enhanced with Fresnel Lenses. *Physical Science International Journal*. 2021;2021(1):8–22. Available from: https://dx.doi.org/10.9734/psij/2021/v25i130233. doi:10.9734/psij/2021/v25i130233.
33) Steward WG, Kreith F. Stationary concentrating reflector cum tracking absorber solar energy collector: optical design characteristics. *Applied Optics*. 1975;14(7):1509–1509. Available from: https://dx.doi.org/10.1364/ao.14.001509.
34) Nouar H, Tahri T, Benyoucef D, Chiba Y, Denai M, Azizi A. Investigation of Climate Effects on the Performance of Solar Chimney Power Plants Using Numerical and Analytical Models: A Case Study for Chlef, Algeria. *PRZEGLĄD ELEKTROTECHNICZNY*. 2021;1(3):115–120. Available from: https://dx.doi.org/10.15199/48.2021.03.22.
35) Ali AS, Djaouida B, Benmachiche AH, Aouachria Z. Abdelmoumène Hakim Benmachiche & Zeroual Aouachria, Performance analysis of a solar chimney power plant system in two Algeria regions. *International Journal of Ambient Energy*. 2021. Available from: https://doi.org/10.1080/01430750.2021.1922500.
36) Moctar M, Maurice TS, Ky A, Konfé B, Dianda. Salifou Ouédraogo DJB. Natural Convection Modeling in a Solar Tower. *Indian Journal of Science and Technology*;2021(48):3475–3493. Available from: https://doi.org/10.17485/IJST/v14i48.1357.
37) Haaf W, Friedrich K, Mayr G, Schlaich J. Solar Chimneys Part I: Principle and Construction of the Pilot Plant in Manzanares. *International Journal of Solar Energy*. 1983;2(1):3–20. Available from: https://dx.doi.org/10.1080/01425918308909911.
38) Kumar M, Sansaniwal SK, Khatak P. Progress in solar dryers for drying various commodities. *Renewable and Sustainable Energy Reviews*. 2016;55:346–360. Available from: https://dx.doi.org/10.1016/j.rser.2015.10.158.
39) Khidhir DK, Atrooshi SA. Investigation of thermal concentration effect in a modified solar chimney. *Solar Energy*. 2020;206:799–815. Available from: https://dx.doi.org/10.1016/j.solener.2020.06.011.
40) Shahreza AR, Imani H. Experimental and numerical investigation on an innovative solar chimney. *Energy Conversion and Management*. 2015;95:446–452. Available from: https://dx.doi.org/10.1016/j.enconman.2014.10.051.
41) Al-Kayiem HH, Aurybi MA, Gilani SIU, Ismaeel AA, Mohammad ST. Performance evaluation of hybrid solar chimney for uninterrupted power generation. In: Energy;vol. 166. Energy. Elsevier BV. 2019;p. 490–505. Available from: https://dx.doi.org/10.1016/j.energy.2018.10.115.
42) Ouedraogo GWP, Kam S, Sougoti M, Moctar O, Bathiebo DJ. Numerical and Experimental Study of Natural Convection Air Flow in a Solar Tower Dryer. *International Journal of Advanced Engineering Research and Science*. 2017;4(5):111–118. Available from: https://dx.doi.org/10.22161/ijaers.4.5.18.